Overheating of Waspaloy

Utada, Satoshi; Sasaki, Ryo; Reed, Roger C.; Tang, Yuanbo T.

DOI:
10.1016/j.matdes.2022.110911

Document Version
Publisher's PDF, also known as Version of record

Citation for published version (Harvard):
Utada, S, Sasaki, R, Reed, RC & Tang, YT 2022, 'Overheating of Waspaloy: Effect of cooling rate on flow stress behavior', *Materials and Design*, vol. 221, 110911. https://doi.org/10.1016/j.matdes.2022.110911

Materials & Design 221 (2022) 110911

Contents lists available at ScienceDirect

Materials & Design

journal homepage: www.elsevier.com/locate/matdes

Overheating of Waspaloy: Effect of cooling rate on flow stress behavior

Satoshi Utada [a,*], Ryo Sasaki [b], Roger. C. Reed [a,c], Yuanbo. T. Tang [a,*]

[a] Department of Materials, University of Oxford, Parks Road, Oxford OX1 3PH, United Kingdom
[b] Metallurgical Research Laboratory, Hitachi Metals, 1240-2 Hashima-cho, Yasugi-shi, Shimane-ken 692-0014, Japan
[c] Department of Engineering Science, University of Oxford, Parks Road, Oxford OX1 3PJ, United Kingdom

HIGHLIGHTS

- Tensile tests with prior overheating on Waspaloy were performed utilizing precise temperature controlling capability of electro-thermal mechanical testing system.
- Overheating at 1000 °C with a cooling rate of 50 K/s severely decreased tensile properties at 700 °C.
- Significant dissolution of precipitates at 1000 °C is the reason of tensile property loss.
- Sufficient re-precipitation and growth for tensile property can occur during slower cooling at 1 K/s.
- Microstructural response during the thermal history can be observed using in situ resistivity measurement.

GRAPHICAL ABSTRACT

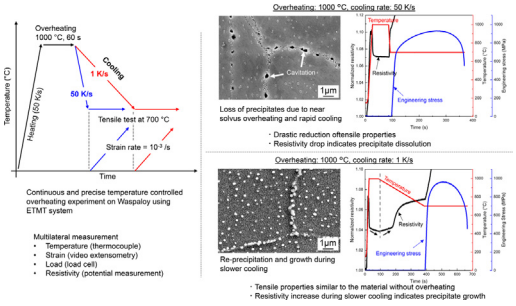

ARTICLE INFO

Article history:
Received 7 April 2022
Revised 21 June 2022
Accepted 29 June 2022
Available online 2 July 2022

Keywords:
Waspaloy
Overheating
Heat treatment
Electro-thermal mechanical testing (ETMT) system
Miniature tensile test
Superalloy

ABSTRACT

During service of a gas turbine engine, components may suffer instant overheating which is a concern to safe operations. Effect of short overheating on the tensile properties of a Ni-based superalloy Waspaloy has been studied due to its significant importance for practical applications. The results have shown that a combination of near supersolvus overheating at 1000 °C with very rapid cooling at a rate of 50 K/s is most detrimental case to the tensile properties of the material. This is attributed to the absence of γ' and carbide re-precipitation and growth during cooling period. Microstructure change during overheating and cooling has been deduced using in-situ resistivity measurements. This work provides evidence that multilateral measurements including resistivity can shed light on the failure controlling parameters.

1. Introduction

Nickel-based superalloys are a class of high temperature material employed for the hot section of jet engines and industrial gas turbines [1]. The structural integrity is delivered by its long term microstructure stability and its superior resistance to time-dependent deformation and environmental degradation, such as

* Corresponding authors.
E-mail addresses: satoshi.utada@materials.ox.ac.uk (S. Utada), yuanbo.tang@materials.ox.ac.uk (Y.T. Tang).

https://doi.org/10.1016/j.matdes.2022.110911
0264-1275/

creep, fatigue and oxidation. The mechanical properties of Ni-based superalloys are evaluated usually by tensile/compressive test with a monotonic strain rate at a fixed temperature, isothermal creep test, and fully reversed or tensile fatigue test. To take into account of operating condition that is more representative during service, complex instrumentation can be carried out to interrogate the behavior of thermo-mechanical fatigue, dwell fatigue, and non-isothermal creep properties.

A crucial challenge for superalloys during engine operation is overheating of the turbine section, an event which is not uncommon. Short and instant overheating can occur in contingency power operation of aero-engines, such as single engine operation (so-called One Engine Inoperative, OEI regime), emergency landing abort, and rapid acceleration in military operation. For example, the tip of a turbine blade can be exposed to overheated temperature as high as 1260 °C [2], which is more than 200 °C higher than its designed temperature. Studies on overheating effect have been performed predominantly for alloys designed for blade applications [3–8], where overheating usually emerges. Only limited literature has addressed this issue for lower $\gamma\prime$ containing alloys, for example, disk and sealing applications. In fact, sealing failure in high pressure turbine section can lead to cooling air leakage, which ultimately leads to uncontained failures which is unfortunately fatal [9].

From the background explained above, the overheating effect on Waspaloy was assessed against the tensile yielding behaviour at 700 °C, which is strongly linked to the low cycle fatigue performance–the failure mode of sealing rings. Waspaloy is still one of the most heavily used superalloys for disk and sealing rings [10] despite the fact that it is a typical cast & wrought superalloy that first entered into service in 1950s [11]. Although it has been studied extensively [12–14], there is still a need to understand the abnormal scenarios for better life predictions and failure analyses. Due its industrial relevance, high temperature behaviors of Waspaloy are studied in recent publications as well [15,16]. Three critical overheating parameters, including overheating temperature, cooling rate from overheating, and holding time before loading were examined using an Instron electro-thermal mechanical testing (ETMT) system. The innovative device allows for in-situ monitoring of $\gamma\prime$ evolution and integrated instant heat treatment & testing capability, hence any influence coming from 'quenched & reheated' is avoided. Consequences of specific thermal history are discussed with relevance to microstructure characteristics using resistivity measured throughout the test. This work examines the materials' tolerance to abnormal operation from an industrial-design relevant perspective.

2. Experimental Methods

2.1. Experimental material: Waspaloy

Round bars of Waspaloy was acquired from Neonickel (UK) obtaining a dimension of 16.4 mm in diameter and 200 mm in length, where the analyzed chemical composition (provided by supplier) is given in Table 1. The material prior to machining was fully heat treated in three steps, i.e. 1010 °C/4 h/water quench (solution anneal), 843 °C/4 h/air quench (stabilization) and 760 °C/16 h/air quench (aging). As characterized, the parent grain size (disregard twins) is ~35 μm exhibiting no dominating texture.

Table 1
Analyzed chemical composition of Waspaloy (Ni bal.).

Elements	wt%	Elements	wt%
Co	12.33	B	0.005
Cr	19.5	Cu	0.02
Al	1.33	Mn	0.01
Fe	1.44	Si	0.02
Mo	3.81	Zr	0.05
Ti	3.02	P	0.004
C	0.04	N_2	0.0023

To decide overheating temperature for this study, ThermoCalc equilibrium simulation using TTNI8 database and differential scanning calorimetry (DSC) using NETZSCH DSC 404 F1 Pegasus were conducted. Waspaloy sample having a 3 mm × 3 mm × 1 mm dimension and surface polished to P4000 grit SiC abrasive paper was prepared for DSC and the sample was placed in a Pt crucible. DSC was operated with a heating rate of 0.17 K/s (10 K/min) and argon atmosphere. Specific heat capacity C_p of Waspaloy was obtained by calibration using a sapphire piece having similar mass to the Waspaloy sample, heated in the same Pt crucible. The $\gamma\prime$ solvus of the material was determined as 1044 °C according to DSC measurement shown in Fig. 2. The simulated $\gamma\prime$ solvus is 1022 °C (Fig. 1), which is reasonably accurate. DSC and simulated values are given in Table 2. To compare the DSC result and resistivity response of the material during heating, one sample was heated at 0.17 K/s (same rate as DSC) in ETMT system and resistivity was measured. Detail of ETMT system is described in the following subsection.

2.2. Tensile tests with overheating using ETMT system

Mechanical properties with application of overheating is measured by judicious use of an Instron ETMT system with a 5 kN load cell. The machine has an integration of two control channels for simultaneous command of mechanical deformation and temperature [17], which allows a simulation of thermal history of the processing route and assessment of the associated properties [18]. The specimens were extracted from the bars using electric discharge machining (EDM) into dogbone shape of 40 mm length, where the cross-sectional area in the gauge section is 1 × 1 mm^2. The specimen is then grounded using abrasive media up to 4000 grit and then spot-welded at the center with a K-type thermocouple for control of temperature. A K-type thermocouple generally can be used temperatures up to 1260 °C and its accuracy is greater of 2.2 °C or 0.75% in ANSI standard. The specimen is heat up using direct current by Joule's effect that enables a heating and cooling rate of 100 K/s. The water-cooled grips are placed 16 mm apart to develop an equilibrium temperature distribution ~3 mm at the centre, which is considered as the gauge section [19]. Strain development is evaluated using an iMetrum non-contact video extensometry system. To enable tracking of local displacement, speckle patterns were applied on the specimen surface using VHT flame proof high temperature spray paint. Image data was acquired at a frequency of 10 fps and subsequently analysed using the VideoGauge software package [20].

The testing program is illustrated schematically in Fig. 3. Overheating is typically performed separately to high temperature mechanical test as shown in Fig. 3(a) [4]. In this study, ETMT system is utilized to perform overheating and tensile test sequence without interrupting high temperature environment Fig. 3(b). Each test is consisted by two parts: (1) free expansion with overheating and cooling and (2) isothermal deformation at 700 °C. Three key variables of industrial relevance were explored to account for thermal history effect on deformation, namely overheating temperature (900 & 1000 °C), cooling rate (1 & 50 K/s) and holding time (5 & 1000 s).

Overheating temperatures were decided from thermal analysis result as previously shown in Fig. 2, where 1000 °C can be described as a temperature slightly below the $\gamma\prime$ solvus. Cooling rates are chosen to as an upper and lower bound of the cooling rate

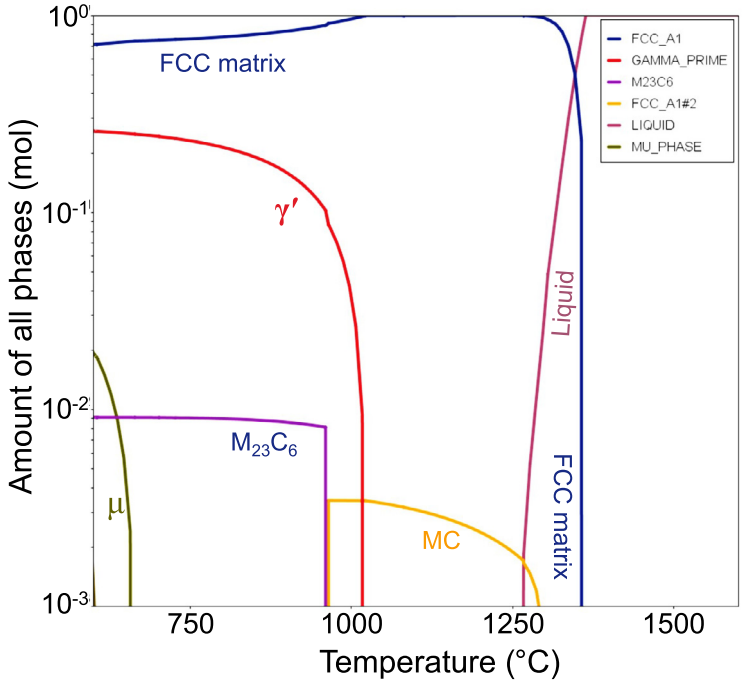

Fig. 1. Equilibrium phase diagram of Waspaloy between 600–1600 °C obtained using ThermoCalc software with TTNI8 database.

Table 2
Comparison of DSC thermal analysis result and ThermoCalc simulation using TTNI8 database.

	DSC (°C)	TTNI8 (°C)
Liquidus	1369	1364
Solidus	1287	1266
MC	-	1304
$\gamma\prime$	1044	1022
$M_{23}C_6$	-	964
σ/μ	598	664

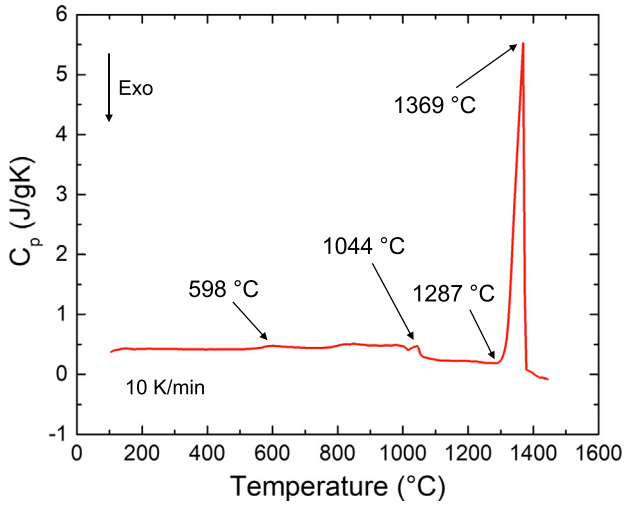

Fig. 2. DSC profile of Waspaloy at heating rate of 0.17 K/s (10 K/min).

that might occur in the real situation. Cooling rate at component surface is typically 5 K/s in case of air cooling [21] , and this value may increase to some extent if forced convection applies. On the other hand, cooling rate for the bulk part is in the order of 1 K/s, which has been used in many studies [22–24]. The details of thermal history can be found in Table 3. The overheated specimens were also compared to the reference materials, i.e. without overheating. Three repeats were completed in each condition for statistical significance.

2.3. In-situ resistivity measurement

In addition to thermocouple for controlling temperature, two wires made by Ni95(Al + Mn + Si)5 used as potential contacts were spot welded 1.5 mm away from each side of the thermocouple for resistivity measurement to account for the 3 mm gauge section. For the calculation of the resistivity, sample's cross-sectional area was measured by micrometer and the length was fixed to 3 mm. Before heating up to overheating temperature, samples were dwelled for 5 s at 150 °C to avoid instant ramp up of a current. Resistivity value at the dwelling temperature of 150 °C was used to normalize the obtained resistivity. The resistivity was used for strain measurement in other studies using ETMT system [19]. However, in this study, the resistivity change will be used to interpret evolution of $\gamma\prime$ precipitation and phase transition during prior overheating sequence where external load was absent [17,19,25,26]. This enables in-situ monitoring of microstructure change throughout overheating and cooling period before applying tensile deformation, in a non-destructive manner.

2.4. Microstructure characterization

Microstructure of the material after testing were characterised using a Zeiss Merlin field emission gun scanning electron microscope (FEG-SEM). The images were acquired at an acceleration voltage of 15 kV and probe current of 5 nA. To better reveal the microstructure, in particular the $\gamma\prime$ precipitate, electrolytic etching was employed for post metallography preparation using 15% phosphoric acid at 3 V DC. Secondary electron (SE) micrographs were collected for each sample after deformation.

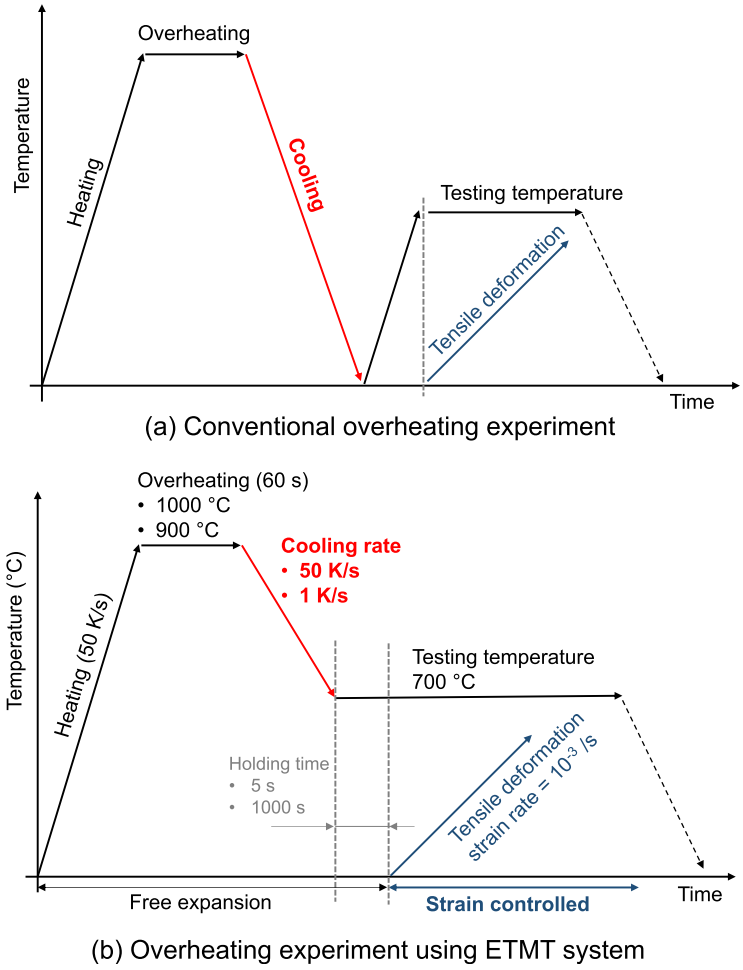

Fig. 3. Testing diagram showing temperature history of a specimen. (a) Conventional overheating experiment. (b) Overheating experiment in this study using ETMT system.

Table 3
Summary of prior overheating conditions and tensile test results.

Name	Prior overheating				Tensile test at 700 °C, strain rate = 10^{-3}/s		
	Heating rate (K/s)	Temperature (°C)	Cooling rate (K/s)	Dwell time (s)	0.2% proof stress (MPa)	Ultimate tensile strength (MPa)	Strain at failure (%)
NoOH	50	-	-	5	885	1028	36
1000–50	50	1000	50	5	646	849	18
1000–50-D	50	1000	50	1000	665	893	25
1000–1	50	1000	1	5	785	992	40
900–50	50	900	50	5	754	945	36

* Result values are averages of three tests.

3. Results

3.1. Resistivity during monotonic heating

Resistivity during monotonic heating at a rate of 0.17 K/s was measured using electric current and voltage up to 1200 °C and shown in Fig. 4 with the same DSC profile which was shown previously in Fig. 2. Four peak temperatures are identified and labeled to the resistivity curve in Fig. 4. In Fig. 4, one can see that initially resistivity increases as temperature increases, a common behavior for metallic material [17]. Bottom peak of resistivity at 1023 °C is assumed to be complete dissolution of γ' phase as the precipitate is usually a source of resistance [17]. Before the temperature reaches the solvus, resistivity decreases and increases again, creating two upper peaks. First upper peak at 568 °C corresponds to onset of σ/μ dissolution, which is in good agreement with DSC profile. Second upper peak is onset of γ' dissolution. This is also indicated by unstable DSC profile starting around 800 °C up to γ' solvus.

Direct comparison of DSC thermal analysis and resistivity measurement using same heating rate shows corresponding responses created by phase transformation of the material.

3.2. Tensile tests with prior overheating

Tensile tests with different prior overheating and cooling histories were successfully performed using the ETMT system. The results of the tensile tests are illustrated in Fig. 5(a, b), and summa-

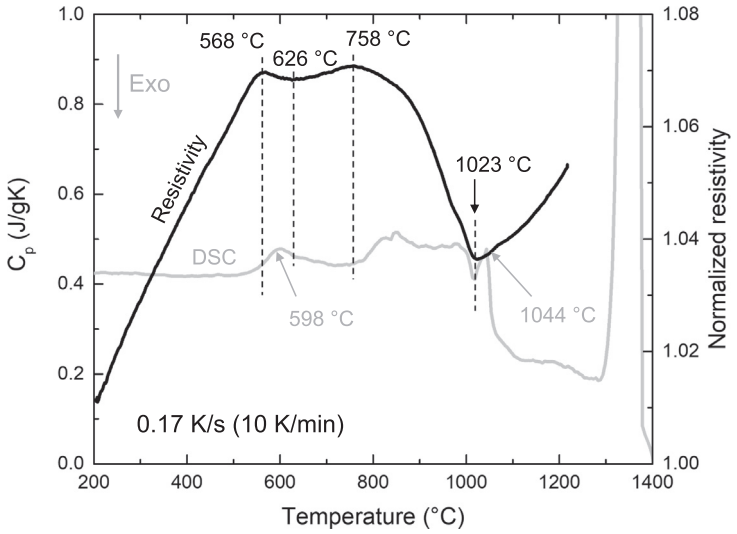

Fig. 4. DSC profile and normalized resistivity of Waspaloy at heating rate of 0.17 K/s (10 K/min).

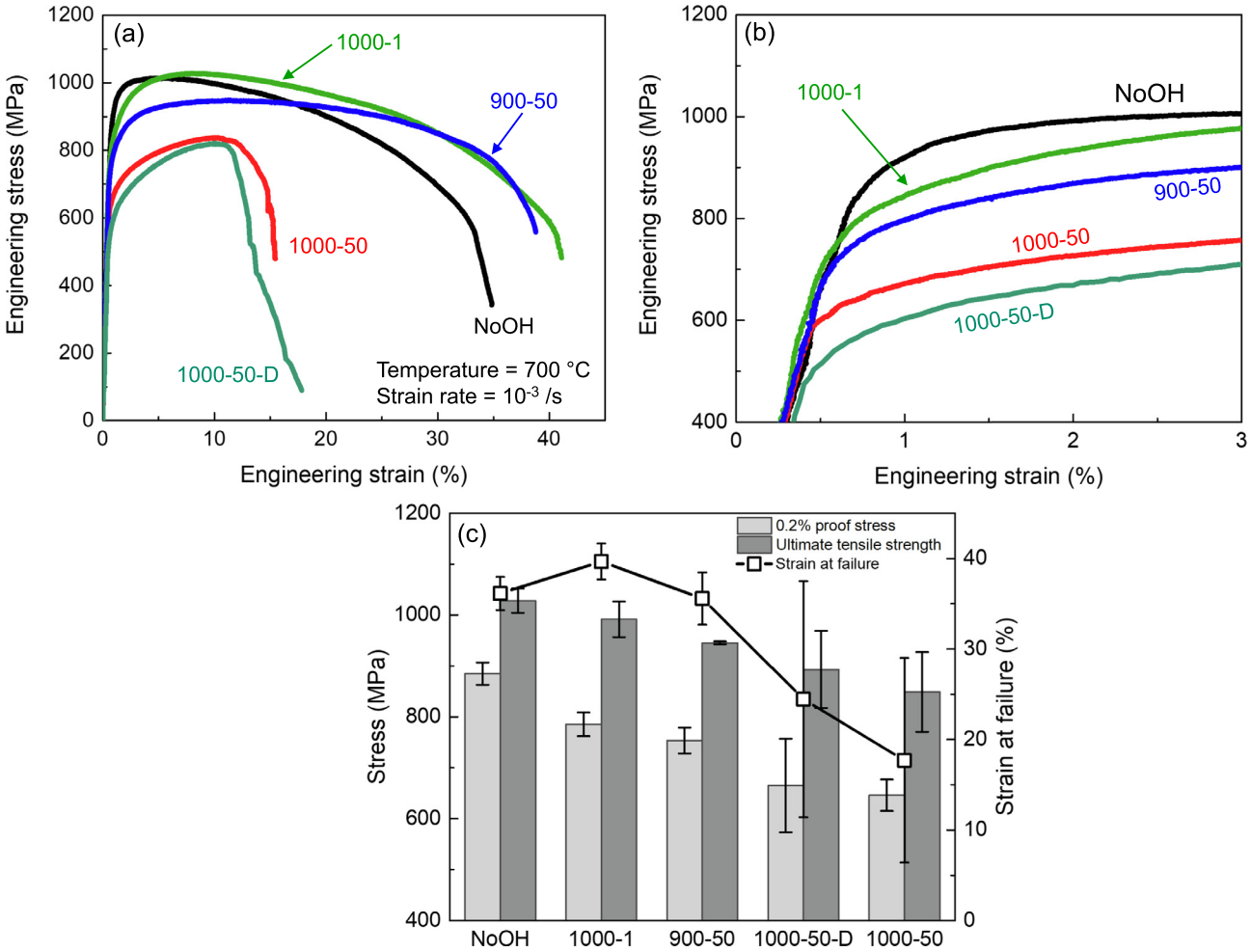

Fig. 5. Tensile test results of Waspaloy tested at 700 °C and strain rate at 10^{-3}/s with different prior overheating and cooling histories. (b) is a magnified scale of (a). 0.2 % proof stress, ultimate tensile strength, and strain at failure are summarized in (c).

rized in Table 3 and Fig. 5(c). Compared to the reference specimen labeled as NoOH in Fig. 5, overheating had the effect of decreasing the flow stress in all cases. Of all the conditions examined, an overheating at 1000 °C with fast cooling rate of 50 K/s (1000–50 and 1000–50-D) conferred the most detrimental effect on the material's yield strength. Ductility of 1000–50 and 1000–50-D varied large including ones showing much lower value compared to that of material without overheating (Fig. 5(a)). Dwelling at 700 °C for

1000 s before applying tensile load resulted in having identical proprieties to the test with a short dwell of 5 s. Specimens with lower overheating temperature (900 °C, 900–50) or slower cooling rate (1 K/s, 1000–1) showed decreased yield stress compared to the reference; however, overall tensile properties were not heavily affected.

3.3. Resistivity during overheating and tensile test

The normalized resistivity of a deformed section was calculated and plotted with temperature and engineering stress in Fig. 6. Fig. 6 proves that temperature was accurately controlled within ±3 °C from the target temperature during the test, including heating and cooling periods. In the same figure, engineering stress is plotted as a function of testing time. Because the test was performed in displacement controlled mode, testing time indirectly represents strain of a specimen, and hence, a stress–time curve has similar shape to a stress–strain curve.

All resistivity profiles in Fig. 6 show similar features as Fig. 4 including two upper peaks during heating up to overheating target of 900 or 1000 °C and resistivity drop after reaching target temperatures. During overheating at 1000 °C, resistivity showed slight decreasing trend for three materials 1000–50 (Fig. 6(a), 1000–50–D (Fig. 6(b)), and 1000–1 (Fig. 6(c)) and start increasing again during cooling period. Faster cooling conditions (cooling rate 50 K/s, Fig. 6(a)) present very short period of increasing resistivity. During dwell at 700 °C in Fig. 6(b), resistivity increased until 200 s, and decreased slightly until the start of the tensile deformation. When the material was subjected to the slower cooling (cooling rate 1 K/s, Fig. 6(d)), resistivity start increasing with very small slope at 990 °C as indicated by dotted line, and shows large jump after 909 °C creating saturated curve like dwelling in 1000–50-D. For the lower overheating condition, resistivity gradually decreases after reaching 900 °C (Fig. 6(d)) and become stable at certain point. Magnitude of increasing resistivity for 900–50 during cooling is the smallest of all. Resistivity increases during the elastic regime of the tensile deformation, and the resistivity slope changes to higher increasing rate for the plastic regime. Similar resistivity behaviors were observed during tensile deformation for all specimens regardless of prior overheating conditions.

The first derivative of resistivity is plotted in Fig. 7 and was used to estimate the temperature that changes the resistivity curve drastically. Since the heating rate up to overheating temperature is same for all conditions, all profiles are showing same feature until two peaks (24 s) during heating sequence. For 50 K/s cooling rate (1000–50), resistivity started increasing at 87.5 s which corresponds to 943 °C, followed by the large jump at 88.6 s / 892 °C (Fig. 7(a)). Similar behavior was observed for 1000–50-D as this sample has the same temperature control steps as 1000–50 (Fig. 7(b)). If a specimen was cooled slower at 1 K/s, very small resistivity increment started at 94.2 s / 990 °C and large jump started at 176.2 s / 909 °C (Fig. 7(c)). Small increase of resistivity started at 86.6 s / 791 °C during cooling sequence of 900–50 Fig. 7(d). Dotted lines in Fig. 7 are indicating initiating point of tensile deformation which is expressed as increase of resistivity that corresponding to straining of the measured section.

3.4. Microstructure analyses

The microstructures of specimens after tensile testing were observed at an area 0.5 mm away from the fracture surface. Representative precipitate scale microstructure images are shown in Fig. 8. The original material without any overheating (Fig. 8(a)) had two size distribution of intragranular γ' precipitates, intergranular primary γ', and carbides which were confirmed by energy dispersive X-ray spectroscopy (not presented here). The bimodal intragranular precipitation size distribution has been reported in Waspaloy and similar class of alloys in different studies [12,27,28,13]. Lower temperature overheating at 900 °C (900–50, Fig. 8(b)) and overheating at 1000 °C with slower cooling at 1 K/s (1000–1, Fig. 8(c)) had similar precipitate distribution to the original material without overheating (NoOH). A rapid cooling at 50 K/s from 1000 °C shown as Fig. 8(d, e) had the least quantity of visible secondary γ' precipitates (diameter between 50–150 nm) inside grains compared to other specimens. Furthermore, tertiary γ' precipitates were observed inside grains of all specimens except for 1000–50 in Fig. 8(e). Materials having overheating at 1000 °C with cooling rate of 50 K/s (Fig. 8(e, f)) had cavitation along grain boundaries that spread all over the deformed section as shown in Fig. 8 (d). 1000–50 and 1000–50-D had less connectivity of intergranular primary γ' precipitates and carbides compared to other three materials after the tensile tests. Comparison of these microstructures confirms that overheating at 1000 °C dissolved large fraction of γ' precipitates and carbides in the Waspaloy used in this study, and 50 K/s cooling rate was fast enough to prevent significant re-precipitation and growth of these precipitates.

4. Discussion

To the authors' best knowledge, this is the first study that has analyzed the effect of an overheating on the material's mechanical proprieties, in a consecutive process with accurate temperature control. The advantages of the ETMT system has been effectively utilized to achieve this complex test with in situ resistivity measurement that helps to understand microstructural behavior during the prior overheating. Mechanical properties of overheated Waspaloy and validation by the multi-scale measurement are discussed further in this section.

4.1. Effect of prior overheating on precipitate morphology

As mentioned in the introduction, previous studies on the effect of overheating have concentrated mainly on blade alloys at subsolvus [5,6] or incipient melting temperature [3,29]. For example, prior supersolvus overheating has been performed by Tong et al. for cast and wrought Ni-based superalloy; this showed that short supersolvus overheating decreases material's tensile and creep properties [4]. Another study by Andersson et al. has shown effect of different sub to supersolvus heat treatment temperatures on Waspaloy to understand material's ductility above 900 °C [13]. In the study by Andersson et al., significant loss of ductility was reported after supersolvus treatment at 1080 °C due to a dissolution of γ' and $M_{23}C_6$ precipitates.

In the present study, microstructure of the 1000–50 specimen after the deformation (Fig. 8(d, e)) indicates that overheating at 1000 °C promotes dissolution of γ' phase, and faster cooling rate of 50 K/s prevented growth of γ' precipitates. Dissolution of γ' precipitates was expected from DSC (Fig. 2), ThermoCalc simulation (Fig. 1), resistivity measurement (Fig. 4), and the alloy's original solution treatment temperature of 1010 °C. Strength of this type of superalloys is known to be determined by size and distribution of γ' precipitates [27,14,30,31]. Therefore, it can be readily understood that the decreased tensile strength of 1000–50 specimen is due to the absence of intragranular secondary γ' precipitates, consistent with previous study by Tong et al. [4]. Because 1000–50-D did not show significant difference in tensile properties compared to that of 1000–50, precipitate growth during longer dwell for 1000 s at 700 °C is assumed to be sluggish that it had only a minor contribution to the microstructure evolution (Fig. 8(f)). Indeed, standard aging treatment of Waspaloy requires heat treatment at 843 and 760 °C for much longer duration to generate ideal precip-

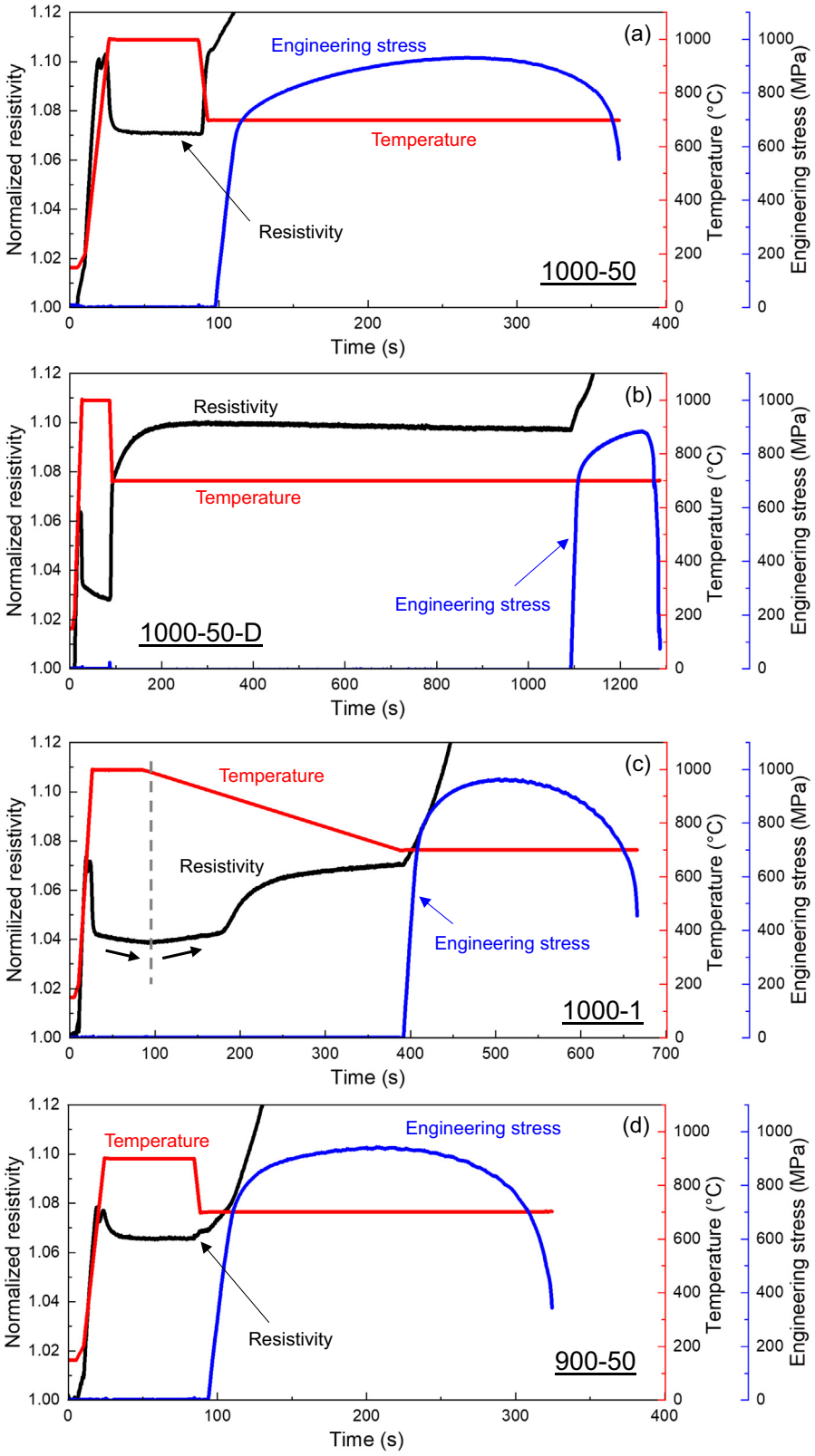

Fig. 6. Diagrams showing relationship of resistivity, temperature, and engineering stress to time of an experiment. (a) Overheating at 1000 °C and cooling rate at 50 K/s (1000–50). (b) Overheating at 1000 °C and cooling rate at 50 K/s followed by 1000 s of dwell at 700 °C (1000–50-D). (c) Overheating at 1000 °C and cooling rate at 1 K/s (1000–1).Dotted line is indicating transition of resistivity decreasing to increasing. (d) Overheating at 900 °C and cooling rate at 50 K/s (900–50)..

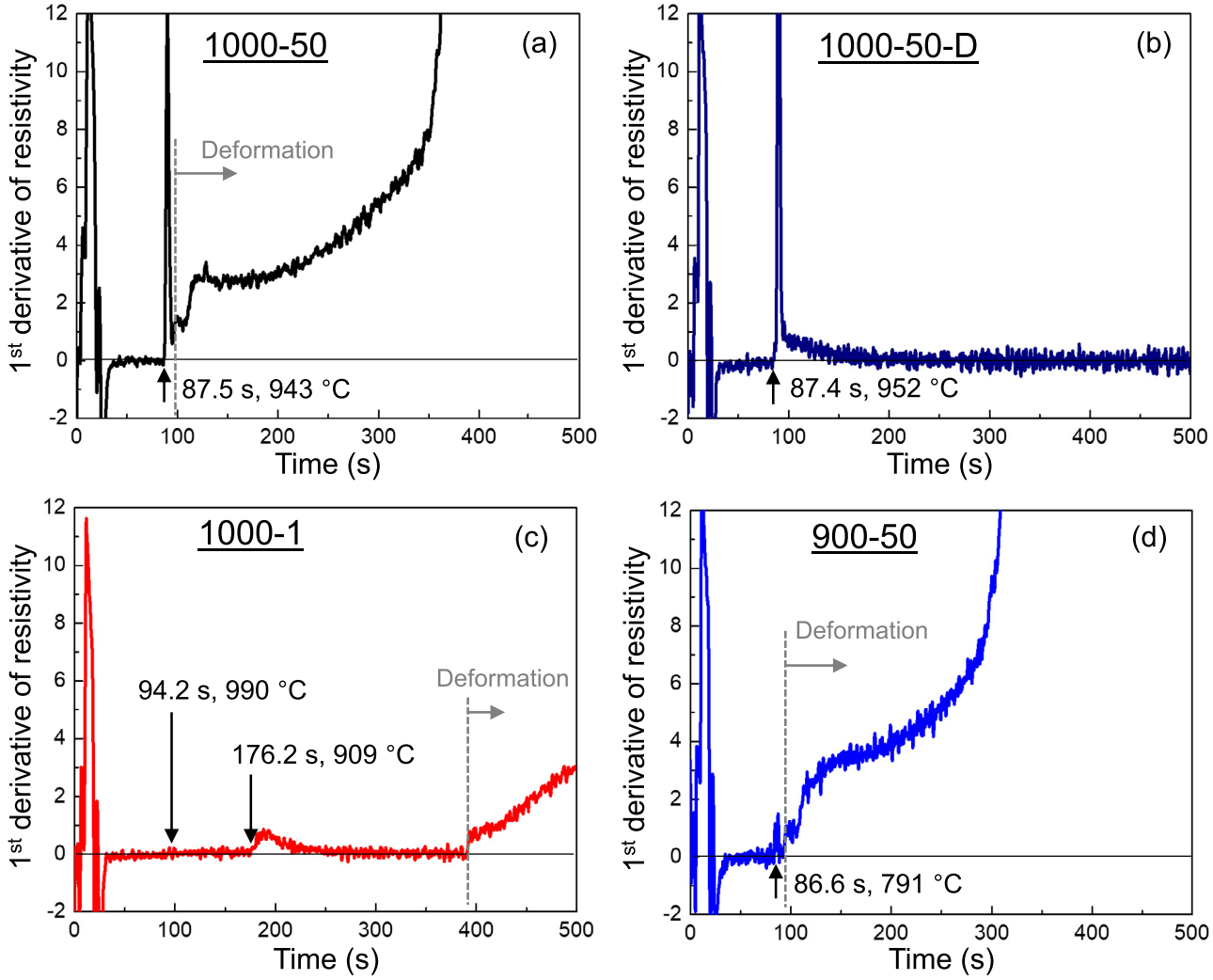

Fig. 7. First derivative of resistivity curve of is plotted as a function of a time. Original resistivity curves of 1000–50 (1), 1000–50-D (b), 1000–1 (c), and 900–50 (d), are from Fig. 6(a), Fig. 6(b), Fig. 6(c), and Fig. 6(d), respectively. Dotted lines are indicating initiating point of tens.ile deformation.

itate mythologies. Such observations are also in accordance with the previous study showing 700 °C is too low to develop effective quantity of $\gamma\prime$ precipitate [4].

Indeed, cavitation in the grain boundaries (Fig. 8(d-f)) can also contribute to the property degradation, which was reported in the study by Andersson et al. [13]. Identifying a solvus of $M_{23}C_6$ is difficult from DSC result due to unsteadiness between 800–1000 °C (Fig. 4), however, it is likely that absence of intergranular primary $\gamma\prime$ and carbides are caused by near-solvus overheating at 1000 °C and the rapid cooling at 50 K/s. Intergranular cavitation can be considered as a reason of ductility loss for 1000–50 and 1000–50-D. However, as the size of an error bar for overheated materials in Fig. 5 shows, the ductility is not constant in three test results. Reason behind this large scatter can be related to a slight decrease in temperature measurement accuracy of K-type thermocouple at 1000 °C (0.75% by ANSI standard) as explained in the experimental section. ±7.5 °C at this temperature potentially influences intergranular microstructure drastically [16]. Therefore, deeper characterization is necessary for clear explanation to the large ductility scatter of 1000–50 and 1000–50-D.

4.2. Understanding microstructure transition by resistivity response

The importance of the present study is that specimen's cooling rate from the overheating temperatures is controlled precisely with measuring the resistivity. This controlled experiment provides details of what has occurred during heating/cooling steps, which is important information for industrial purposes.

The data in Fig. 7 and Fig. 4 can be used to rationalize the material's microstructural response during the thermal history. Normalized resistivity in Fig. 4 and Fig. 6(c) are plotted together in Fig. 9. The resistivity drop starting at 868 °C during over heating period in Fig. 9 mainly corresponds to dissolution of $\gamma\prime$ precipitates as reported in studies using CMSX-4 single crystal Ni-bases superalloy [17,19]. The following resistivity decrease during overheating period suggests that $\gamma\prime$ precipitates continue to dissolve at this time. As labeled in Fig. 7, temperature at which resistivity starts increasing again is 943 and 952 °C for 1000–50 and 1000–50-D, respectively. The temperature at which resistivity increases is higher (990 °C) when the cooling rate is lower (1 K/s). Increasing resistivity is indeed representing growth of $\gamma\prime$ precipitates. However, at the same time, the temperature that resistivity increases is lower for 50 K/s, meaning that effect of undercooling had been captured here in case of 1000–50 and 1000–50-D. Resistivity jump indicated in Fig. 7(c) at 176.2 s (909 °C) is initiation of regime having sluggish $\gamma\prime$ growth behavior. Saturation of resistivity during dwell after 250 s for 1000–50-D (Fig. 6(b), Fig. 7(b)) suggests microstructure evolution at 700 °C is limited, which agrees with the tensile test result showing identical properties to 1000–50 regardless of dwell time (see Fig. 5). Slower cooling rate at 1 K/s

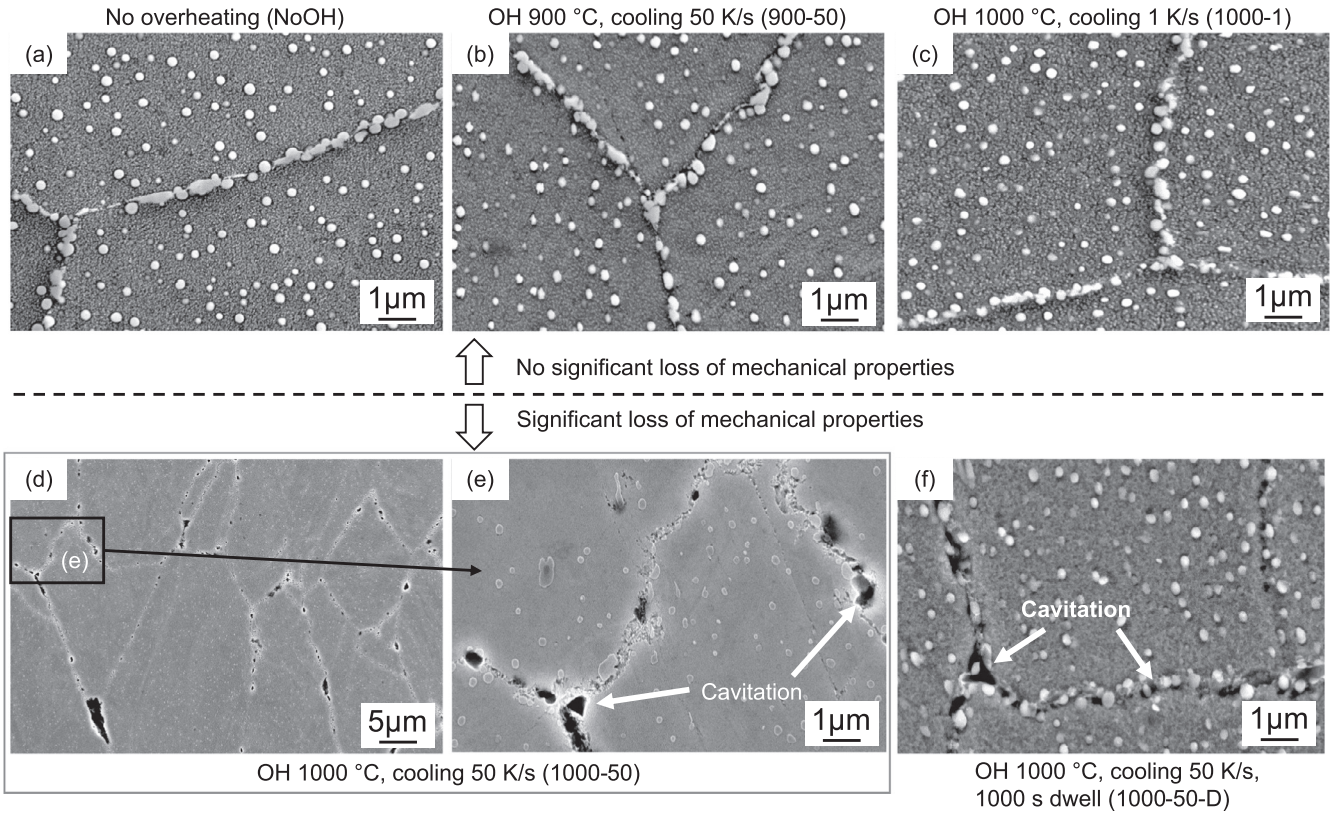

Fig. 8. Microstructures of Waspaloy after a tensile test at 700 °C. (a) No overheating (NoOH). (b) Overheating at 900 °C and cooling rate at 50 K/s (900–50). (c) Overheating at 1000 °C and cooling rate at 1 K/s (1000–1). (d, e) Overheating at 1000 °C and cooling rate at 50 K/s (1000–50), lower (d) and higher (e) magnifications. (f) Overheating at 1000 °C and cooling rate at 50 K/s, followed by dwell at 700 °C for 1000 s before tensile test (1000–50-D). White arrows are pointing at cavitation in grain boundaries.

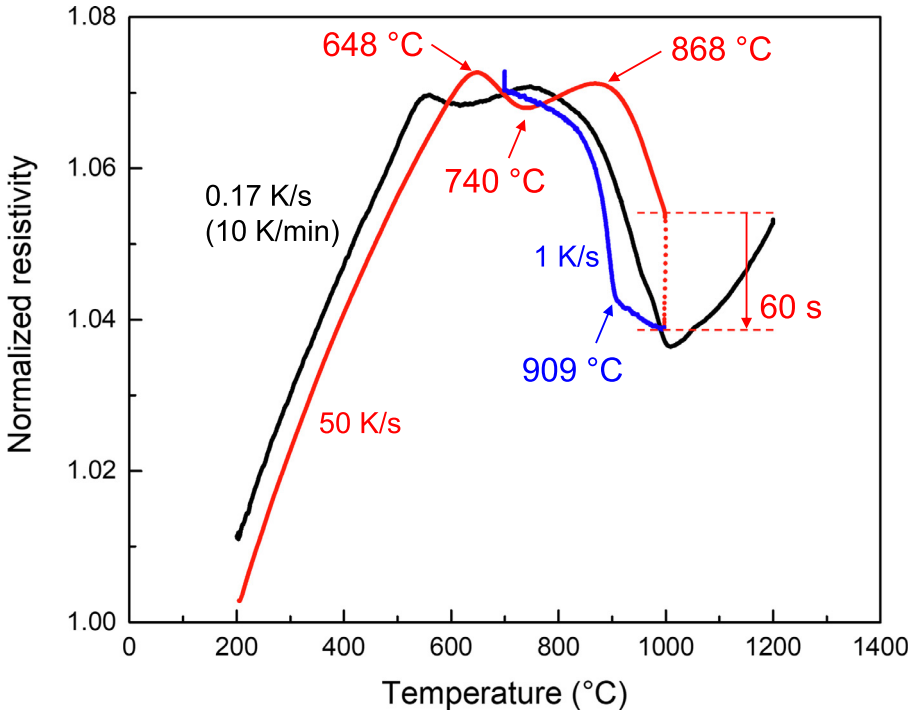

Fig. 9. Resistivity of Waspaloy measured using ETMT system with different heating rate 0.17 K/s and 50 K/s. 1000–1 sample before tensile deformation has heating rate at 50 K/s (red curve), holding at 1000 °C for 60 s (red dotted line), and cooling at 1 K/s (blue curve).

(Fig. 6(d) has gradual resistivity increase after reaching 990 °C, large change of slope at 909 °C, and this stops at around 830 °C. These pieces of information suggest that re-precipitation and growth of γ' and/or $M_{23}C_6$ precipitates can proceed rather rapidly at approximately between 830∼900 °C.

Cooling rate during heat treatment of superalloys and other alloys is known to be important to achieve desired material properties. Hence, many studies have concentrated upon understanding microstructural responses and consequent mechanical properties in many different cooling conditions [12,22–24,32,33]. For example, the study on Waspaloy by Groh et al. was with maximum cooling rate from supersolvus temperature in order of 1 K/s [12]. In such studies, precipitation and evolution of γ' phase during the cooling were evaluated, and faster cooling rate is generally suggested for controlling microstructure in subsequent aging treatments to achieve desired mechanical properties [12,28,32]. This scenario only applies when the material is subjected to multiple heating steps in longer time scale compared to the present study.

By way of contrast, the present study considers the overheating to near solvus temperature of superalloy component during operation. Controlled cooling rate provides evidence that if a material is cooled too fast, it can cause instant degradation of mechanical properties. When a subsequent aging treatment is not applied, cooling rate should be in a range that is not too fast for precipitation and growth, but not too slow to avoid exceeded precipitate coarsening. The result showed that 1 K/s cooling rate is slow enough for re-precipitation/growth and thus restored the mechanical properties significantly. The ETMT system is capable of performing temperature controlled experiment which is very useful to understand material behavior in specific conditions. This has strong advantage in designing a component for high temperature applications. In fact, the result of the present study suggests that overheating may not be an issue if a material is slowly cooled (1 K/s) or if the overheating does not exceed solvus temperature, overheating at 900 °C in this case.

4.3. Multilateral measurement in the ETMT system

Resistivity measurement in the ETMT system has been used to either measure magnitude of strain during mechanical test or quantify dissolution and precipitation of γ' phase in individual purposes. Continuous experiments in this study that focused use of resistivity for in situ microstructure analysis was very useful to indirectly follow microstructure evolution during testing. By using reference data of resistivity response during straining or precipitation, it is possible to detect in much more complex situation, such as under condition which temperature and stress change at the same time, like thermomechanical fatigue test.

Although microstructure evolution was minimal when the material was cooled rapidly at 50 K/s (Fig. 8(e)), resistivity was strongly affected once the temperature reaches 892 °C as shown in Fig. 6(a) and Fig. 7(a). The explanation could be that either a very small quantity of precipitate has large influence on the resistivity, or else the existence of nano-scale precipitate that was not able to be observed in the SEM. Careful post experiment observation using higher resolution technique needs to be designed to explain the detail of microstructure evolution mechanisms and resistivity responses of the material.

In the future, in order to use resistivity really efficiently to deduce information about microstructure, influence of different factors must be investigated, i.e. different grain size, textured grains, dislocation densities, single crystal superalloy with carbides, different compositions, and topologically closed-packed (TCP) and other phases. All these can show different effect on the material's resistivity. For example, Darnbrough et al. used nanocrystalline material to show a grain size effect during heating of a material [34]. Correlation with measured data and post test microstructure can also help to design new heat treatment conditions. Further understanding on these relations should improve acquisition of more information through all testing period in the ETMT system.

5. Conclusions

The effect of instant overheating with rapid heating and cooling on tensile properties of Waspaloy has been studied by utilizing an electro-thermal mechanical testing (ETMT) system with the ability to perform complex thermal history tests. The followings are the main conclusions derived from this work:

1. Overheating at 1000 °C for 60 s with a cooling rate of 50 K/s drastically decreased tensile properties of Waspaloy at 700 °C. Decreased overheating temperature (900 °C) or decreased cooling rate (1 K/s) had less effect on the material's tensile properties.
2. Microstructure analyses showed that γ' precipitates in Waspaloy significantly dissolve at 1000 °C in less than 60 s. Faster cooling rate of 50 K/s down to 700 °C preserves a near-precipitate free microstructure and decreases yield strength of the material. On the other hand, γ' phase can grow sufficiently during slower cooling (1 K/s) from 1000 °C, which resulted in overheated Waspaloy having similar tensile properties of reference one without overheating.
3. Precipitate dissolution and re-precipitation/growth during rapid heating and cooling can be indirectly detected by measuring resistivity of heated section, without interrupting the test. A potential of multilateral property evaluation of the ETMT system has been demonstrated.

Data availability

Data will be made available on request.

Declaration of Competing Interest

The authors declare that they have no known competing financial interests or personal relationships that could have appeared to influence the work reported in this paper.

Acknowledgments

Authors acknowledges financial support from Hitachi Metals - University of Oxford UTC (University Technology Centre). Dr. Joseph Ghoussoub (formerly at Department of Materials, University of Oxford) and Andrew Pearce (Instron) are acknowledged for their technical assistance in the experiments. Prof. Graham McCartney (Department of Materials, University of Oxford) is gratefully acknowledged for suggestions.

References

[1] R.C. Reed, The Superalloys: Fundamentals and Applications, Cambridge University Press, Cambridge, 2006, https://doi.org/10.1017/CBO9780511541285.
[2] X. Guo, W. Zheng, C. Xiao, L. Li, S. Antonov, Y. Zheng, Q. Feng, Evaluation of microstructural degradation in a failed gas turbine blade due to overheating, Eng. Fail. Anal. 103 (2019) 308–318, https://doi.org/10.1016/j.engfailanal.2019.04.021.
[3] I.M. Wolff, Precipitation accompanying overheating in nickel-base superalloy, Mater. Charact. 29 (1) (1992) 55–61, https://doi.org/10.1016/1044-5803(92)90096-ZISTEX.
[4] J.Y. Tong, K. Yagi, Y.R. Zheng, Q. Feng, Microstructural degradation and its corresponding mechanical property of wrought superalloy GH4037 caused by very high temperature, J. Alloy. Compd. 690 (2017) 542–552, https://doi.org/10.1016/j.jallcom.2016.08.081.

[5] J. Cormier, M. Jouiad, F. Hamon, P. Villechaise, X. Milhet, Very high temperature creep behavior of a single crystal Ni-based superalloy under complex thermal cycling conditions, Philos. Mag. Lett. 90 (8) (2010) 611–620, https://doi.org/10.1080/09500839.2010.489887.
[6] S. Antonov, W. An, S. Utada, X. Guo, C. Schwalbe, W. Zheng, C.M. Rae, J. Cormier, Q. Feng, Evaluation and comparison of damage accumulation mechanisms during non-isothermal creep of cast Ni-based superalloys, in: S. Tin, M. Hardy, J. Clews, J. Cormier, Q. Feng, J. Marcin, C. O'Brien, A. Suzuki (Eds.), Superalloys 2020, Springer International Publishing, 2020, pp. 228–239, https://doi.org/10.1007/978-3-030-51834-9_22.
[7] W. Xing, G. Zhu, X. Zuo, X. Guo, Z. Zhao, H. Xiao, Z. Zheng, W. Zhao, C. Liu, Abnormal creep property degradation in a directionally solidified superalloy DZ406 after suffering overheating, Mater. Charact. 173 (2021) 110910, https://doi.org/10.1016/j.matchar.2021.110910.
[8] S. Utada, L. Després, J. Cormier, Ultra-High Temperature Creep of Ni-Based SX Superalloys at 1250 C, Metals 11 (10) (2021) 1610, https://doi.org/10.3390/met11101610.
[9] J.J. Pardee, Airworthiness Directives; General Electric Company GE90 Series Turbofan Engines, Fed. Reg. 66 (188) (2001) 49326–49328. URL https://www.federalregister.gov/documents/2001/09/27/01-24274/airworthiness-directives-general-electric-company-ge90-series-turbofan-engines.
[10] R.E. Chupp, R.C. Hendricks, S.B. Lattime, B.M. Steinetz, Sealing in Turbomachinery, J. Propul. Power 22 (2) (2006) 313–349, https://doi.org/10.2514/1.17778.
[11] C.T. Sims, A history of superalloy metallurgy for superalloy metallurgists, Superalloys 1984 (1984) 399–419, https://doi.org/10.7449/1984/Superalloys_1984_399_419.
[12] J.R. Groh, Effect of cooling rate from solution heat treatment on waspaloy microstructure and properties, Superalloys 1996 (1996) 621–626, https://doi.org/10.7449/1996/Superalloys_1996_621_626.
[13] J. Andersson, G.P. Sjöberg, L. Viskari, M. Chaturvedi, Effects of different solution heat treatments on the hot ductility of superalloys, Mater. Sci. Technol. 29 (1) (2013) 43–53, https://doi.org/10.1179/1743284712Y.0000000108.
[14] K.-M. Chang, X. Liu, Effect of γ' content on the mechanical behavior of the WASPALOY alloy system, Materials Science and Engineering: A 308 (1) (2001) 1–8, https://doi.org/10.1016/S0921-5093(00)02042-6ISTEX.
[15] A. Agnoli, C. Le Gall, J. Thebault, E. Marin, J. Cormier, Mechanical Properties Evolution of γ'/γNickel-Base Superalloys During Long-Term Thermal Over-Aging, Metall. Mater. Trans. A 49 (9) (2018) 4290–4300, https://doi.org/10.1007/s11661-018-4778-x.
[16] H. Liu, L. Zheng, D. Wang, X. Wei, H. Min, Y. Jin, Q. Tai, Dissolution and Coarsening Kinetics of γ' Precipitates in Waspaloy during Solution Treatment at Temperatures of 1000–1045 C, J. of Materi Eng and Perform (2022), https://doi.org/10.1007/s11665-022-06768-7.
[17] B. Roebuck, D. Cox, R. Reed, The temperature dependence of γ' volume fraction in a Ni-based single crystal superalloy from resistivity measurements, Scripta Mater. 44 (6) (2001) 917–921, https://doi.org/10.1016/S1359-6462(00)00662-XISTEX.
[18] Y.T. Tang, N. D'Souza, B. Roebuck, P. Karamched, C. Panwisawas, D.M. Collins, Ultra-high temperature deformation in a single crystal superalloy: Mesoscale process simulation and micromechanisms, Acta Mater. 203 (2021) 116468, https://doi.org/10.1016/j.actamat.2020.11.010.
[19] B. Roebuck, D.C. Cox, R.C. Reed, An innovative device for the mechanical testing of miniature specimens of superalloys, in: K.A. Green, T.M. Pollock, H. Harada, T.E. Howson, R.C. Reed, J.J. Schirra, S. Walston (Eds.), Superalloys 2004, The Minerals, Metals, & Materials Society, 2004, pp. 523–528. doi:10.7449/2004/Superalloys_2004_523_528.
[20] S. Sulzer, E. Alabort, A. Németh, B. Roebuck, R. Reed, On the Rapid Assessment of Mechanical Behavior of a Prototype Nickel-Based Superalloy using Small-Scale Testing, Metall. Mater. Trans. A 49 (9) (2018) 4214–4235, https://doi.org/10.1007/s11661-018-4673-5.
[21] D. Dye, K.T. Conlon, R.C. Reed, Characterization and modeling of quenching-induced residual stresses in the nickel-based superalloy IN718, Metall. Mater. Trans. A 35 (6) (2004) 1703–1713, https://doi.org/10.1007/s11661-004-0079-7.
[22] S. Milenkovic, I. Sabirov, J. LLorca, Effect of the cooling rate on microstructure and hardness of MAR-M247 Ni-based superalloy, Mater. Lett. 73 (2012) 216–219, https://doi.org/10.1016/j.matlet.2012.01.028.
[23] M. Li, J. Coakley, D. Isheim, G. Tian, B. Shollock, Influence of the initial cooling rate from γ' supersolvus temperatures on microstructure and phase compositions in a nickel superalloy, J. Alloy. Compd. 732 (2018) 765–776, https://doi.org/10.1016/j.jallcom.2017.10.263.
[24] P. Caron, T. Khan, Improvement, Materials Science and Engineering 61 (2) (1983) 173–184, https://doi.org/10.1016/0025-5416(83)90199-4.
[25] N. D'Souza, B. Roebuck, D.M. Collins, G.D. West, C. Panwisawas, Relating micro-segregation to site specific high temperature deformation in single crystal nickel-base superalloy castings, Materials Science and Engineering: A 773 (2020) 138862, https://doi.org/10.1016/j.msea.2019.138862.
[26] N. D'Souza, M.C. Hardy, B. Roebuck, W. Li, G.D. West, D.M. Collins, On the Rate Dependence of Precipitate Formation and Dissolution in a Nickel-Base Superalloy, Metall. Mater. Trans. A 53 (7) (2022) 2480–2495, https://doi.org/10.1007/s11661-022-06680-8.
[27] M.P. Jackson, R.C. Reed, Heat treatment of UDIMET 720Li: the effect of microstructure on properties, Materials Science and Engineering: A 259 (1) (1999) 85–97, https://doi.org/10.1016/S0921-5093(98)00867-3ISTEX.
[28] R. Radis, M. Schaffer, M. Albu, G. Kothleitner, P. Pölt, E. Kozeschnik, Multimodal size distributions of γ' precipitates during continuous cooling of UDIMET 720 Li, Acta Mater. 57 (19) (2009) 5739–5747, https://doi.org/10.1016/j.actamat.2009.08.002.
[29] L.S. Araujo, C.H. de Melo, R.P. Gonçalves, A. de Vasconcelos Varela, L.H. de Almeida, The effect of a very high overheating on the microstructural degradation of superalloy 718, Journal of Materials Research and Technology 8 (1) (2019) 683–689, https://doi.org/10.1016/j.jmrt.2018.03.006.
[30] R.W. Kozar, A. Suzuki, W.W. Milligan, J.J. Schirra, M.F. Savage, T.M. Pollock, Strengthening Mechanisms in Polycrystalline Multimodal Nickel-Base Superalloys, Metall. Mater. Trans. A 40 (7) (2009) 1588–1603, https://doi.org/10.1007/s11661-009-9858-5.
[31] T. Osada, N. Nagashima, Y. Gu, Y. Yuan, T. Yokokawa, H. Harada, Factors contributing to the strength of a polycrystalline nickel–cobalt base superalloy, Scripta Mater. 64 (9) (2011) 892–895, https://doi.org/10.1016/j.scriptamat.2011.01.027.
[32] S. Steuer, Z. Hervier, S. Thabart, C. Castaing, T.M. Pollock, J. Cormier, Creep behavior under isothermal and non-isothermal conditions of AM3 single crystal superalloy for different solutioning cooling rates, Materials Science and Engineering: A 601 (2014) 145–152, https://doi.org/10.1016/j.msea.2014.02.046.
[33] S.A. Sajjadi, H.R. Elahifar, H. Farhangi, Effects of cooling rate on the microstructure and mechanical properties of the Ni-base superalloy UDIMET 500, J. Alloy. Compd. 455 (1) (2008) 215–220, https://doi.org/10.1016/j.jallcom.2007.01.091ISTEX.
[34] J.E. Darnbrough, B. Roebuck, P.E.J. Flewitt, The influence of temperature and grain boundary volume on the resistivity of nanocrystalline nickel, J. Appl. Phys. 118 (18) (2015) 184302, https://doi.org/10.1063/1.4935290.